

# Quantitative Assessment of Tumor Oxygen Dynamics: Molecular Imaging for Prognostic Radiology

Ralph P. Mason,<sup>1\*</sup> Sophia Ran,<sup>2</sup> and Philip E. Thorpe<sup>2</sup>

<sup>1</sup>Department of Radiology, U.T. Southwestern Medical Center, Dallas, Texas

<sup>2</sup>Department of Pharmacology, U.T. Southwestern Medical Center, Dallas, Texas

---

**Abstract** One of the fundamental molecules governing the survival of mammalian cells is oxygen. Oxygen has gained particular significance in tumor developmental biology and oncology. An increasingly diverse array of methods is now available to characterize tumor oxygenation. This Prospect will consider a new method, Fluorocarbon Relaxometry using Echo planar imaging for Dynamic Oxygen Mapping (*FREDOM*), which we have recently developed for oximetry, examine application to a specific therapeutic example and place this technique in the context of other approaches. *J. Cell. Biochem. Suppl.* 39: 45–53, 2002. © 2002 Wiley-Liss, Inc.

**Key words:** magnetic resonance imaging; hexafluorobenzene; oxygen; tumor; tissue factor; antibody targeting

---

The human genome has been sequenced and it is now realized that cells are ultimately characterized by gene expression and proteomics, which govern phenotype. There is also an increasing realization that environmental factors (epigenetic) can strongly influence cell development and response to therapy. This is particularly relevant to oncology. It has long been appreciated that hypoxic tumor cells are more resistant to radiotherapy [Gray et al., 1953]. Indeed, a threefold increase in radio resistance may occur when cells are irradiated under hypoxic conditions compared with  $pO_2 > 15$  Torr for a given single radiation dose. However, recent modeling has indicated that the proportion of cells in the range 0–20 Torr may be most significant in terms of surviving a course of fractionated radiotherapy [Wouters and Brown,

1997]. Increasingly, there is evidence that hypoxia also influences such critical characteristics as angiogenesis, tumor invasion, and metastasis [Höckel and Vaupel, 2001; Knowles and Harris, 2001]. Moreover, repeated bouts of intermittent hypoxic stress may be important in stimulating tumor progression [Cairns et al., 2001]. Thus, the ability to measure  $pO_2$  non-invasively, and repeatedly, with respect to acute or chronic interventions becomes increasingly important.

Early work examined cells in vitro, where ambient oxygen concentrations are readily controlled. In vivo, hypoxia may be achieved by clamping the blood supply to a tumor, but other levels of oxygenation reflect the interplay of supply and consumption. Robust fine needle polarographic electrodes opened the possibility of measuring  $pO_2$  in tumors in situ in vivo to define local  $pO_2$  under baseline conditions or with respect to interventions. In early work, Cater and Silver [Cater and Silver, 1960] showed the ability to monitor  $pO_2$  at individual locations in patient's tumors with respect to breathing oxygen. Later, Gatenby et al. [1988] showed that  $pO_2$  in a tumor was correlated with clinical outcome. Tumor oximetry received its greatest boost with the development of the Eppendorf Histogram polarographic needle electrode system. This computer-controlled device equipped with a stepper motor can reveal distributions of tumor oxygenation and has

---

Grant sponsor: The National Cancer Institute; Grant numbers: RO1 CA74951, CA54168, CA79515; Grant sponsor: Cancer Imaging Program; Grant number: P20 CA 86354; Grant sponsor: NIH BRTP Facility; Grant number: P41-RR02584.

\*Correspondence to: Ralph P. Mason, PhD, C. Chem, Department of Radiology, U.T. Southwestern Medical Center, 5323 Harry Hines Blvd., Dallas, TX 75390-9058. E-mail: Ralph.Mason@UTSouthwestern.edu

Received 4 October 2002; Accepted 8 October 2002

DOI 10.1002/jcb.10404

Published online in Wiley InterScience (www.interscience.wiley.com).

© 2002 Wiley-Liss, Inc.

been applied extensively to clinical trials. Many reports have now shown that tumors are highly heterogeneous and have extensive hypoxia: strong correlations have been shown in cervix and head and neck tumors between median  $pO_2$  or hypoxic fraction and survival or disease free survival [Brizel et al., 1996; Höckel et al., 1996; Nordmark et al., 1996; Fyles et al., 1998]. Thus, tumor oxygenation is now recognized as a strong prognostic indicator and this device has laid a convincing foundation for the value of measuring  $pO_2$  in patients. However, the Histogram is highly invasive and it is not possible to make repeated measurements at individual locations, precluding dynamic studies to assess the influence of interventions on tumor  $pO_2$ .

Thus, many other techniques have been developed to assess tumor oxygenation more or less directly (Table I) [Stone et al., 1993]. Magnetic resonance methods are attractive, since MR is inherently non-invasive. The pioneering work of Thomas [1988] showed that tissue  $pO_2$  could be imaged in various organs based on the  $^{19}F$  NMR spin-lattice relaxation rate (R1) of perfluorocarbon reporter molecules following i.v. infusion. Prompted by these studies, we surveyed a number of PFCs and identified that hexafluorobenzene (HFB, Fig. 1) has many virtues as a  $pO_2$  reporter [Mason et al., 1996]. Symmetry provides a single narrow  $^{19}F$  NMR signal and the spin lattice relaxation rate is highly sensitive to changes in  $pO_2$ , yet minimally responsive to temperature. From a

**TABLE I. Comparison of Tumor Oximetry Techniques**

Technique	Reporter	Parameter measured	Invasiveness	Spatial characteristic	Temporal resolution	References
Oximetry <i>FREDOM</i>	Hexafluorobenzene (perfluorocarbon)	R1	Minimally 32 G needle	Map multiple locations each 4 mm <sup>3</sup>	6.5 min	[Hunjan et al., 2001; Zhao et al., 2001a, 2002a,b]
$^{19}F$ MRS	Perfluorocarbon	R1	i.v.	Perfused regions	1 s to 6.5 min	[Mason et al., 1994]
ESR/EPR	Charcoal Nitroxides	Linewidth	23 G needle i.t.	Single location	Seconds	[Stone et al., 1993]
PEDRI	Free radical	OverHauser	i.v.	Global or map	Seconds	
Needle electrode (Histogram)	Oxygen	Enhancement Current	26 G needle	Cubic millimeter maps	10 min	
	Oxygen	Current	26 G needle	Single location	~1 s	[Cater and Silver, 1960; Gatenby et al., 1988; Zhao et al., 2002b; Mason et al., 1999a]
	Oxygen	Current	26 G needle	Multiple tracks	1 s per location	[Brizel et al., 1996; Höckel et al., 1996; Fyles et al., 1998; Mason et al., 1999a]
Optical probe (OxyLite <sup>TM</sup> , FOXY <sup>TM</sup> )	RhCl <sub>2</sub>	Fluorescent lifetime	26 G needle	Typically 2–4 locations	Real time	[Zhao et al., 2001b]
Phosphorescence	PD complex	Lifetime	i.v.	Maps	<1 min	
Mass spectrometry	Oxygen <sup>a</sup>	Atoms	Needle	Single location		
Vascular oxygenation						
NIR	Hemoglobin <sup>a</sup>	HbO <sub>2</sub> /Hb	Non-invasive	Global	Real time	[Liu et al., 2000]
BOLD	Hemoglobin <sup>a</sup>	HbO <sub>2</sub> /Hb	Non-invasive	Maps	1–5 s	[Howe et al., 1999]
Cryospectro photometry	Hemoglobin <sup>a</sup>	HbO <sub>2</sub> /Hb	Biopsy	Microscopic	Once	[Stone et al., 1993]
Hypoxia						
Histology	Nitroimidazoles Pimonidazole	%Tissue stained	i.v. + biopsy	Microscopic	Once	[Stone et al., 1993]
SPECT	EF5	%Tissue stained	i.v. + biopsy	Microscopic	Once	[Stone et al., 1993]
PET	LAZA	Photon counts	i.v.	Maps		[Ballinger, 2001]
	EF5	Positron decays	i.v.	Maps		[Ballinger, 2001]
	Cu-ATSM	Positron decays	i.v.	Maps		[Ballinger, 2001]
Indirect methods						
$^{31}P$ NMR	PCr, ATP, Pi <sup>a</sup>	Phosphorylation potential	Non-invasive	2–10 cc	> 10 min	[Stone et al., 1993]
COMET	DNA strand breaks <sup>a</sup>	Electrophoretic migration	Biopsy	Cellular	Once	[Stone et al., 1993]

<sup>a</sup>Endogenous.

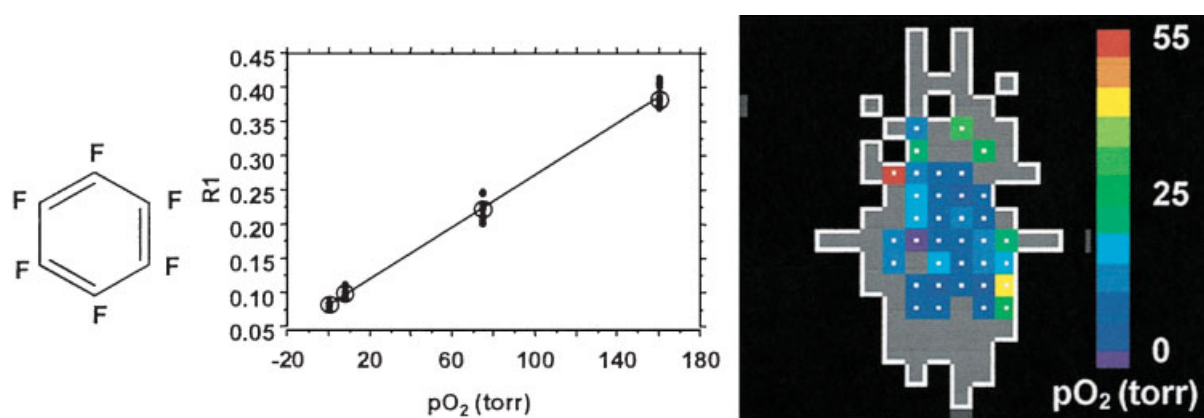


Fig. 1. Hexafluorobenzene, the linear oxygen dependence of the  $^{19}\text{F}$  NMR spin-lattice relaxation rate (R1) and a typical  $\text{pO}_2$  map from a Hodgkin's lymphoma xenograft in a SCID mouse.

practical perspective, HFB is readily available commercially in high purity, cheap and well characterized in terms of lack of toxicity [Zhao et al., 2001a]. Indeed, HFB exhibits no mutagenicity, no teratogenicity or fetotoxicity and the manufacturer's material data safety sheet indicates  $\text{LD}_{50} > 25 \text{ g/kg}$  (oral-rat) and  $\text{LC}_{50} 95 \text{ g/m}^3$  per 2 h (inhalation-mouse).

Recognizing that tumors are heterogeneous and that  $\text{pO}_2$  may fluctuate, we developed a procedure, which allows repeated quantitative maps of regional  $\text{pO}_2$  to be achieved with multiple individual locations simultaneously in 6.5 min with a precision of 1–3 Torr when  $\text{pO}_2$  is in the range 0–15 Torr [Hunjan et al., 2001]. We have applied *FREEDOM* to diverse tumor types and interventions [Hunjan et al., 2001; Zhao et al., 2001a,b, 2002a,b; Song et al., 2002], as discussed in detail below, but here we describe the assessment of a human tumor xenograft with respect to respiratory challenge and administration of a vascular targeting agent.

## METHODS

Human L540 Hodgkin's tumors were implanted subcutaneously in the flanks of male CB17 severe combined immunodeficient (SCID) mice and allowed to grow to  $\sim 1.5 \text{ cm}$  diameter (3–6 mm thick). Mice were anesthetized using ketamine/xylazine. HFB ( $\sim 40 \mu\text{l}$ , Lancaster) was injected directly in both central and peripheral regions of the disc-like tumors using a Hamilton syringe (Reno, NV) with a custom made fine sharp needle (32 G) using our standard procedure [Zhao et al., 2001b]. Each mouse was placed within a 2 cm single turn solenoid

coil in an Omega CSI 4.7 T horizontal bore magnet system with actively shielded gradients. Proton and  $^{19}\text{F}$  MR images were obtained to confirm the distribution of HFB. Tumor oxygenation was estimated on a regional basis using  $^{19}\text{F}$  echo planar imaging (EPI) relaxometry of the HFB [Hunjan et al., 2001]. Briefly, following a pulse burst saturation recovery (PBSR) preparation sequence with a variable recovery time ( $\tau$ ), a single spin echo planar image was acquired. Applying the ARDVARC protocol (Alternated Relaxation Delays with Variable Acquisitions to Reduce Clearance effects) [Hunjan et al., 2001] enhanced the quality of the relaxation data, and typically a precision of 2–5 Torr at each of 20–50 voxels was achieved within a tumor in 6.5 min. The spin-lattice relaxation rate ( $R1 = 1/T1$ ) was calculated for each voxel using a three-parameter fit of signal intensity  $y_i = A(1 - (1 + W)\exp(-R1 \cdot \tau_i))$  by the Levenberg–Marquardt least-squares algorithm. Selection criteria were applied to the data: data were accepted provided that the relative standard error of T1 ( $\sigma T1/T1 < 25\%$  and  $0 < \sigma T1 < 2.0 \text{ s}$ ). Oxygen tension was estimated using the relationship  $\text{pO}_2 \text{ (Torr)} = 7.6 \times (R1 - 0.077 + 0.00009T) / (0.018 - 0.00017T)$ , where T is rectal temperature in  $^\circ\text{C}$  and R1 is the spin-lattice relaxation rate in  $\text{s}^{-1}$  [Le et al., 1997].

The inhaled gas could be manipulated via a nose cone from air to carbogen (95%  $\text{O}_2$ /5%  $\text{CO}_2$ ;  $1 \text{ dm}^3/\text{min}$ ). In other cases, the air-breathing mice were injected i.v. with anti-VCAM1-tTF (truncated tissue factor) coaguligand ( $200 \mu\text{l} = 40 \mu\text{g}$  protein) to produce tumor-specific infarct [Huang et al., 1997]. The coaguligand was

constructed by conjugating the MK2.7 monoclonal antibody directed against mouse VCAM-1 to the extracellular domain of human tissue factor (TF), as described previously [Ran et al., 1998]. Thrombosis of tumor vessels was verified histologically in experiments parallel to NMR [Ran et al., 1998]. Briefly, mice were selected at specific time points before and after administration of coaguligand, anesthetized and perfused with heparinized saline. The tumors were removed, fixed in saline and paraffin embedded. Sections were cut, stained with hematoxylin-eosin and the number of thrombosed vessels counted.

Statistical significance of changes in oxygenation was assessed using analysis of variance (ANOVA) on the basis of Fisher PLSD and data are quoted as mean  $\pm$  SE of the mean.

## RESULTS

Typical baseline oxygenation ranged from hypoxia to 50 Torr with mean  $9.7 \pm 1.4$  (SE) Torr and median 7.2 Torr (Fig. 2): no significant changes occurred during three repeat measurements while breathing air over a period of 24 min. Within 8 min of altering the inspired gas to carbogen, there was a change in oxygenation with elevation in mean ( $P < 0.01$ ) and median  $pO_2$ , and decreased hypoxic fraction (Fig. 2). Oxygen tension continued to rise sometimes reaching a plateau after 16 min with mean  $pO_2$  significantly above baseline ( $P < 0.00001$ ). Upon returning the inhaled gas to air, tumor  $pO_2$  gradually declined, but after 24 min was still significantly elevated compared with baseline ( $P < 0.01$ ).

Administration of the anti-VCAM-1.TF coaguligand caused a rapid reduction in  $pO_2$  in well-oxygenated tumor regions (initial  $pO_2 > 10$  Torr) with mean declining from  $15.5 \pm 2.7$  to  $4.2 \pm 2.4$  Torr ( $P < 0.01$ ) after 16 min and to  $-1.5 \pm 2.4$  Torr ( $P < 0.001$ ) after 70 min. Little change was observed in regions, which were initially poorly oxygenated (initial  $pO_2 < 10$  Torr), although some locations indicated increased oxygenation (Fig. 3). Histology showed open blood vessels in the untreated tumors, but substantial thromboses at 4 h.

## DISCUSSION

In the brief experiments described here, we have demonstrated the ability to monitor both baseline  $pO_2$  distributions in a tumor in vivo

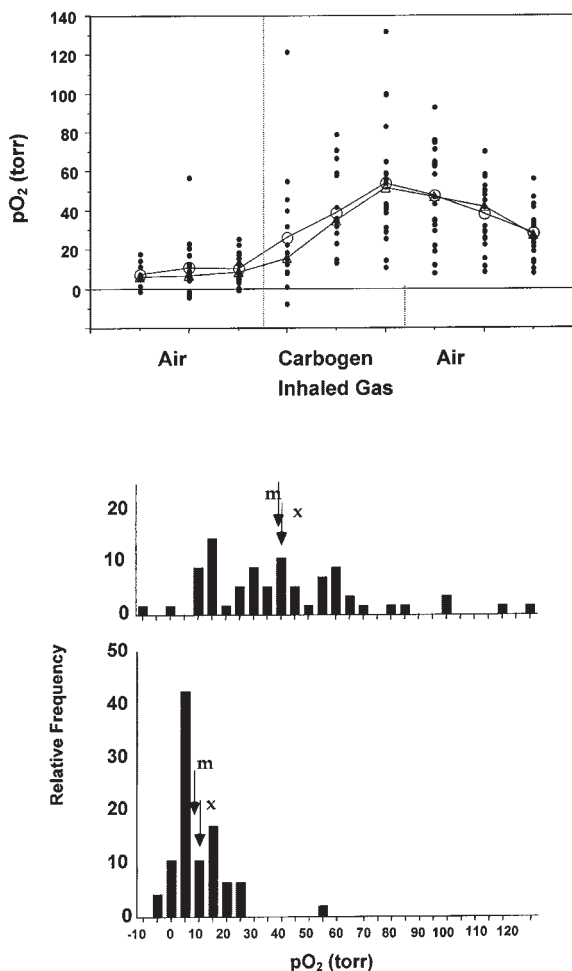


**Fig. 2.** Tumor oxygenation in response to respiratory challenge for human Hodgkin's tumors growing subcutaneously in mice: in each case data have been pooled from three repeat determinations. **Lower:** Histograms of baseline with mouse breathing air. Mean (x)  $pO_2 = 9.7 \pm 1.4$  (SE) Torr, median (m) = 7 Torr. **Center:** Mouse breathing carbogen (95%  $O_2$ /5%  $CO_2$ ): mean  $pO_2 = 41 \pm 3.9$  Torr, median 39 Torr. **Top:** Oxygenation of individual voxels from respective  $pO_2$  maps. The general trend shows increased oxygenation with carbogen and a decline, albeit slower, upon return to breathing air. This emphasizes the need for rapid time resolution and danger of pooling data. Variation in mean ( $\circ$ ) and median ( $\Delta$ )  $pO_2$  with respect to respiratory challenge is overlaid. Each measurement required 6.5 min.

and dynamic changes with respect to interventions. This approach allows multiple specific locations to be interrogated simultaneously and sequentially. The data indicate the importance of temporal and spatial resolution in investigating tumor physiology. During the period of 6.5 min, considerable changes occurred in tumor oxygenation in response to respiratory challenge (Fig. 2). The mapping capability is critical, since it reveals distinct heterogeneity in tumor



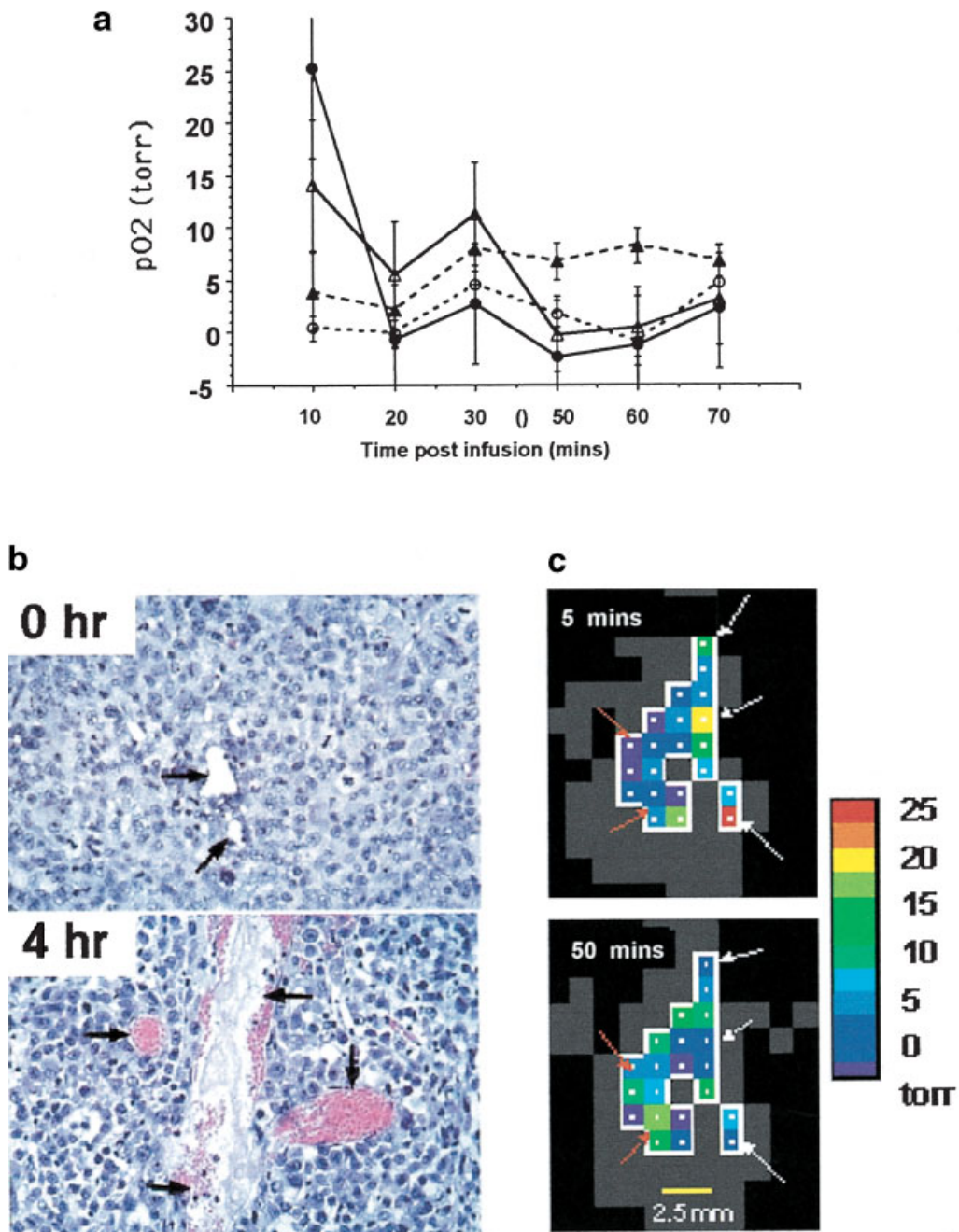


**Fig. 3. a:** Administration of the coaguligand caused a rapid reduction in  $pO_2$  in well-oxygenated tumor regions (initial  $pO_2 > 10$  Torr) with mean declining from  $15.5 \pm 2.7$  to  $4.2 \pm 2.4$  Torr ( $P < 0.01$ ) after 16 min and to  $-1.5 \pm 2.4$  Torr ( $P < 0.001$ ) after 70 min. Considering two representative individual tumor regions (voxels) ● and ▲ with initially high  $pO_2$ , both showed a decline. By contrast, little change was observed in regions, which were initially poorly oxygenated (initial  $pO_2 < 10$  Torr), for

example, ○, although in some regions  $pO_2$  was found to rise significantly ▲. **b:** H & E stained sections show open blood vessels in control tumor, but distinct thromboses 4 h following administration of coaguligand. **c:** Maps of  $pO_2$  obtained using *FREDOM* 5 and 50 min after infusion of coaguligand. Arrows indicate regions showing particularly dramatic decrease or increase in  $pO_2$ .

oxygenation and differential response to intervention. In particular, the initially well-oxygenated regions of the tumor showed a significant decline in  $pO_2$  (hypoxiation) following adminis-

tration of the coaguligand, whereas the less well-oxygenated regions showed minimal response (Fig. 3). This could be attributed to differential vascular efficiency. One would expect

pO<sub>2</sub> to be highest in well-perfused regions and delivery of the coaguligand should also be most efficient there. Meanwhile, less well-oxygenated regions, and hence, by inference less well-perfused regions would tend to be less likely to be infarcted. Indeed, one region (Fig. 3) showed a significant increase ( $P < 0.01$ ) in tumor oxygenation. This could imply diversion of blood to this region resulting from infarct elsewhere. In future, it will be important to correlate pO<sub>2</sub> measurements with blood flow as provided by such non-invasive techniques as <sup>1</sup>H Dynamic Contrast Enhanced (DCE) or Blood Oxygen Level Dependant (BOLD) contrast MRI. The <sup>19</sup>F NMR data are preliminary, but do coincide with histological investigations. Specifically, many, but not all, tumor capillaries were found to be occluded. The great potential advantage of FREDOM over traditional histology is that each tumor serves as its own control, and indeed, individual voxels reveal both baseline heterogeneity and differential response to interventions. Moreover, non-invasive procedures minimize the number of animals and quantity of agent required. Since antibodies may be costly, and difficult to create in large quantities, savings could greatly enhance the efficiency of agent development.

We have previously applied the *FREDOM* approach to various tumor types including syngeneic rat tumors [Mason et al., 1999b; Zhao et al., 2001a,b, 2002a,b]. In diverse sublines of the Dunning prostate R3327 tumor, we have shown distinctly different oxygenation patterns, which were related to tumor differentiation, vascularity, and growth rate [Zhao et al., 2000, 2002b]. Thus, the undifferentiated AT1 subline with volume doubling time of 5 days showed distinct heterogeneity with pO<sub>2</sub> values ranging from > 50 Torr to hypoxia when anesthetized rats breathed air. In response to breathing elevated oxygen (either oxygen or carbogen) those regions initially well oxygenated showed a rapid and significant response, while initially poorly oxygenated regions showed little, if any, response [Hunjan et al., 2001]. The fast growing MAT-Lu subline (VDT 2.7 days) had greater baseline hypoxia and similar response to breathing elevated oxygen [Zhao et al., 2001b, 2002b]. Meanwhile, the moderately well-differentiated HI subline (VDT 9 days) showed very different behavior. Baseline oxygenation was significantly higher, yet a substantial fraction of large tumors was hypoxic. Remarkably,

all regions irrespective of initial pO<sub>2</sub> showed rapid and significant increase in pO<sub>2</sub> with respect to breathing elevated oxygen [Zhao et al., 2002b]. The highly differentiated H tumor (VDT 20 days) had significantly higher baseline oxygenation, but the response to increased oxygen breathing was sluggish compared to HI [Zhao et al., 2000]. Recently, we have also shown application of the technique to mammary 13762NF adenocarcinomas [Song et al., 2002]. Baseline pO<sub>2</sub> was similar to the Dunning prostate AT1, but all regions responded to oxygen intervention, though often slowly with continual increases over 45 min. Such data have suggested that a given tumor type has characteristic baseline pO<sub>2</sub> distributions and response to an intervention. However, baseline pO<sub>2</sub> alone has not been a good indicator of the potential response to an intervention between different tumor types. If such data are confirmed in the clinic, they indicate the potential importance of measuring pO<sub>2</sub> in the tumors of individual patients, so that therapy may be individualized and optimized with inclusion of appropriate adjuvant interventions.

Histogram data have shown value in evaluating baseline pO<sub>2</sub> measurements. In the future, patients may be stratified into well-oxygenated and poorly oxygenated groups for differential therapy. A next step should be the evaluation of the tumors, to see whether their pO<sub>2</sub> can be modulated by a relatively innocuous intervention, such as breathing oxygen. Elevation of tumor oxygenation might bring these hypoxic tumors into the well-oxygenated range and should show an improved response to radiation. Non-responders (persistently hypoxic tumors) could be considered for hypoxia selective cytotoxic therapy, such as tirapazamine [Brown, 1999] in an attempt to render them more sensitive to treatment.

Of greater relevance to the biochemical community is the ability to screen interventions in animals. With the increasing emphasis on speed of development for new therapeutic approaches, non-invasive techniques become increasingly important. As combinatorial approaches gain application, many more agents are available, but typically in small quantities. In the past, assessment of the efficacy of novel coaguligands has relied on histological endpoints (destructive) or gross anatomical evaluation (slow). The *FREDOM* procedure, described here, allows individual locations within a tumor to be followed

for a period of hours. These procedures can be used to rapidly screen new agents and suggest optimal time points for sacrifice and histological evaluation. This will both spare animals and, perhaps more significantly, reduce the amount of drug required. The non-destructive imaging technique will accelerate the discovery process for targets, efficacious conjugates, and successful development of drugs.

As shown in Table I, there are many alternative techniques available to investigate tumor oxygenation. Electrodes have been considered by some to be a “gold standard” and we have shown that  $pO_2$  distributions assessed with the Eppendorf Histogram are commensurate with *FREDOM* [Mason et al., 1999a]. We have also shown similar dynamic response to interventions such as hyperoxic gas inhalation using fiber optic probes or electrodes or *FREDOM* [Zhao et al., 2001b, 2002b]. Electrodes, fiber optic probes, mass spectrometry probes, and many incarnations of ESR require insertion of a sizable needle into tumors and report limited regions raising issues of sampling. While our current implementation of *FREDOM* does require a needle for intratumoral (i.t.) injection, the mobile fluid (HFB) allows a very fine sharp needle (32 G). Moreover, we achieve maps of  $pO_2$  at multiple locations simultaneously. Sampling remains an issue, since we typically interrogate 5–10% of a given tumor volume. However, the highly consistent intertumor behavior between multiple tumors of a given type (and size) suggests appropriate sampling. Moreover, since HFB is highly volatile and clears from tumors within 24 h, repeated measurements on subsequent days for chronic longitudinal investigations requires re-administration of the HFB: the highly consistent data achieved in tumors with such successive measurements indicates the effective representation of the true distribution of oxygen tensions within the tumors [Zhao et al., 2001b]. To avoid violating the tumor itself, reporter molecules can also be delivered i.v. (e.g., oxygen sensitive phosphorescent dyes, ESR sensitive agents, NMR sensitive fluorocarbon emulsions), but such an approach may bias measurements towards vascular oxygenation and particularly towards well-perfused regions of a tumor [Mason et al., 1994; McIntyre et al., 1999].

Specific classes of reporter molecule can reveal hypoxia as a surrogate for  $pO_2$  (e.g., pimonidazole, EF5, CCI-103F) [Stone et al.,

1993]. Following i.v. infusion these agents become reduced in tissues and are trapped. However, in the presence of oxygen, they are reoxidized and ultimately clear from the body. Histological assessment of the distribution of these agents provides microscopic indications of local hypoxia. Both EF5 and pimonidazole are currently being tested in clinical trials. In addition, various labeled derivatives have been developed which are NMR or PET active. Other nuclear imaging agents have been developed specifically to image hypoxia, for example, Cu-ATSM and the galactopyranoside IAZA [Ballinger, 2001].

While many successful reporter molecules have been developed to investigate tumor oxygenation, an alternative approach is to exploit endogenous indicators of oxygenation. Near infrared spectroscopy provides a direct measure of variation in tumor hematocrit (viz. blood volume) and relative hemoglobin oxygen saturation [Liu et al., 2000]. Cheap instrumentation can reveal rapid changes, but current technology provides very coarse spatial resolution, or indeed, global estimates. BOLD contrast MRI approaches provide high spatial and temporal resolution related to hemoglobin oxygen saturation, but signal also responds to variations in vascular volume, and flow [Howe et al., 1999]. Moreover, changes in vascular oxygenation may not coincide with  $pO_2$ , which is a balance between oxygen delivery and consumption and clearance. Ultimately, we must recognize that quantitative estimates of tumor tissue  $pO_2$  have been shown to be directly related to clinical outcome in several tumor types, while other parameters such as vascular oxygenation require further validation in terms of their prognostic value.

Since many biochemical pathways are under oxygen regulation, they can provide an elegant window on hypoxia, for example, induction of Hif-1 and Glut-1 together with secondary responses such as increased production of VEGF, NIP3, and tumor associated macrophage activity [Knowles and Harris, 2001]. While such molecules could themselves indicate hypoxia, a more versatile approach is to adopt the hypoxic response elements as promoter sequences coupled to reporter genes such as GFP (green fluorescent protein) [Cao et al., 2001].

From a clinical perspective,  $^{19}F$  MR remains somewhat esoteric, though the capability can be added to a clinical MR scanner for about \$150k.



For preclinical biochemical studies, NMR systems have routine  $^{19}\text{F}$  capabilities at 4.7, 7, or 9.4 T. Indeed, diverse reporter molecules have been created to access such diverse parameters as transmembrane pH, transmembrane chloride potential,  $[\text{Ca}^{2+}]$ , temperature, and of course pharmacokinetics of drugs such as 5-FU [Mason, 1999].  $^{19}\text{F}$  NMR can also be applied to assess gene therapy, as demonstrated by others, for monitoring the conversions of 5-FC (fluorocytosine) to 5-FU (5-fluorouracil) and by us with the novel class of agent PFONPG as a substrate for  $\beta$ -galactosidase activity [Mason et al., 2002].

Ultimately, the value of a technique depends on its robustness, ease of use, and widespread implementation. To date, few labs had adopted the *FREEDOM* approach because efficient investigation of HFB requires an unusual NMR pulse sequence. With the recent upgrade of our own instrumentation to the Varian Unity INOVA, the software is now available on this popular platform facilitating ready implementation elsewhere. While the *FREEDOM* technique is currently limited to preclinical investigations, we are seeking Investigational New Drug (IND) approval for HFB to facilitate future clinical applications. As with electrode approaches, we foresee initial applications to readily accessible tumors, for example, head and neck, cervical, breast, and prostate. The ability to map  $\text{pO}_2$  in  $<8$  min makes this technique a practical proposition for application to patients, and the value of monitoring dynamic changes in tumor oxygenation has the potential to influence treatment strategies.

In terms of research applications, it is known that tumor tissue  $\text{pO}_2$  varies rapidly in response to many acute interventions ranging from irradiation to photodynamic therapy, various chemotherapies, and experimental new approaches such as vascular targeting agents shown here. We foresee *FREEDOM* as a valuable tool for assessing the dynamic time course of such interventions to provide clear insight into the mode of action of therapeutic approaches and aid in the high throughput screening of new drugs such as vascular targeting and anti-angiogenic agents.

#### ACKNOWLEDGMENTS

This work was supported in part by The National Cancer Institute (RO1 CA74951

(PET), CA54168 (PET), and CA79515 (RPM) and in conjunction with Cancer Imaging Program P20 CA 86354 and NIH BRTP Facility P41-RR02584.

#### REFERENCES

- Ballinger JR. 2001. Imaging hypoxia in tumors. [Review]. *Semin Nucl Med* 31:321–329.
- Brizel DM, Scully SP, Harrelson JM, Layfield LJ, Bean JM, Prosnitz LR, Dewhirst MW. 1996. Tumor oxygenation predicts for the likelihood of distant metastases in human soft tissue sarcoma. *Cancer Res* 56:941–943.
- Brown JM. 1999. The hypoxic cell: A target for selective cancer therapy. *Cancer Res* 59:5863–5870.
- Cairns RA, Kalliomaki T, Hill RP. 2001. Acute (cyclic) hypoxia enhances spontaneous metastasis of KHT murine tumors. *Cancer Res* 61:8903–8908.
- Cao Y, Li C, Zhang X, Dewhirst M. 2001. A study of hypoxia-induced gene expression in human tumors: 48th Annual meeting of Radiation Research. San Juan, PR, p P28–P370.
- Cater D, Silver I. 1960. Quantitative measurements of oxygen tension in normal tissues and in the tumors of patients before and after radiotherapy. *Acta Radiol* 53: 233–256.
- Fyles AW, Milosevic M, Wong R, Kavanagh M-C, Pintile M, Sun A, Chapman W, Levin W, Manchul L, Keane TJ, Hill RP. 1998. Oxygenation predicts radiation response and survival in patients with cervix cancer. *Radiother Oncol* 48:149–156.
- Gatenby RA, Kessler HB, Rosenblum JS, Coia LR, Moldofsky PJ, Hartz WH, Broder G. 1988. Oxygen distribution in squamous cell carcinoma metastases and its relationship to the outcome of radiation therapy. *Int J Radiat Oncol Biol Phys* 14:831–838.
- Gray L, Conger A, Ebert M, Hornsey S, Scott O. 1953. The concentration of oxygen dissolved in tissues at time of irradiation as a factor in radio-therapy. *Br J Radiol* 26: 638–648.
- Howe FA, Robinson SP, Rodrigues LM, Griffiths JR. 1999. Flow and oxygenation dependent (FLOOD) contrast MR imaging to monitor the response of rat tumors to carbogen breathing. *Magn Reson Imaging* 17:1307–1318.
- Huang X, Molema G, King S, Watkins L, Edington TS, Thorpe PE. 1997. Tumor infarction in mice by anti-body directed targeting of tissue factor to tumor vasculature. *Science* 275:547–550.
- Hunjan S, Zhao D, Constantinescu A, Hahn EW, Antich PP, Mason RP. 2001. Tumor oximetry: Demonstration of an enhanced dynamic mapping procedure using fluorine-19 echo planar magnetic resonance imaging in the Dunning prostate R3327-AT1 rat tumor. *Int J Radiat Oncol Biol Phys* 49:1097–1108.
- Höckel M, Vaupel P. 2001. Tumor hypoxia: Definitions and current clinical, biologic, and molecular aspects. *J Natl Cancer Inst* 93:266–276.
- Höckel M, Schlenger K, Aral B, Mitze M, Schäffer U, Vaupel P. 1996. Association between tumor hypoxia and malignant progression in advanced cancer of the uterine cervix. *Cancer Res* 56:4509–4515.
- Knowles HJ, Harris AL. 2001. Hypoxia and oxidative stress in breast cancer. Hypoxia and tumorigenesis. [Review]. *Breast Cancer Res* 3:318–322.



- Le D, Mason RP, Hunjan S, Constantinescu A, Barker BR, Antich PP. 1997. Regional tumor oxygen dynamics:  $^{19}\text{F}$  PBSR EPI of hexafluorobenzene. *Magn Reson Imaging* 15:971–981.
- Liu H, Song Y, Worden KL, Jiang X, Constantinescu A, Mason RP. 2000. Noninvasive investigation of blood oxygenation dynamics of tumors by near-infrared spectroscopy. *Appl Optic* 39:5231–5243.
- Mason RP. 1999. Transmembrane pH gradients in vivo: Measurements using fluorinated vitamin B6 derivatives. *Curr Med Chem* 6:481–499.
- Mason RP, Antich PP, Babcock EE, Constantinescu A, Peschke P, Hahn EW. 1994. Non-invasive determination of tumor oxygen tension and local variation with growth. *Int J Radiat Oncol Biol Phys* 29:95–103.
- Mason RP, Rodbumrung W, Antich PP. 1996. Hexafluorobenzene: A sensitive  $^{19}\text{F}$  NMR indicator of tumor oxygenation. *NMR Biomed* 9:125–134.
- Mason RP, Constantinescu A, Hunjan S, Le D, Hahn EW, Antich PP, Blum C, Peschke P. 1999a. Regional tumor oxygenation and measurement of dynamic changes. *Radiat Res* 152:239–249.
- Mason RP, Constantinescu A, Ran S, Thorpe PE. 1999b. Oxygenation in a human tumor xenograft: Manipulation through respiratory challenge and anti-body directed infarction. *Proc 27th ISOTT*. Dartmouth, NH, p 43.
- Mason RP, Otten P, Li Y, Koeman K. 2002. Gene reporter molecules: A novel approach revealing  $\beta$ -galactosidase activity: ISMRM 10th Scientific Meeting. Honolulu, Hawaii, USA, p 384.
- McIntyre DJO, McCoy CL, Griffiths JR. 1999. Tumour oxygenation measurements by  $^{19}\text{F}$  MRI of perfluorocarbons. *Curr Sci* 76:753–762.
- Nordmark M, Overgaard M, Overgaard J. 1996. Pretreatment oxygenation predicts radiation response in advanced squamous cell carcinoma of head and neck. *Radiother Oncol* 41:31–39.
- Ran S, Gao B, Duffy S, Watkins L, Rote N, Thorpe PE. 1998. Infarction of solid Hodgkin's tumors in mice by antibody-directed targeting of tissue factor to tumor vasculature. *Cancer Res* 58:4646–4653.
- Song Y, Constantinescu A, Mason RP. 2002. Dynamic breast tumor oximetry: The development of prognostic radiology. *Technol Cancer Res Treat* (in press).
- Stone HB, Brown JM, Phillips T, Sutherland RM. 1993. Oxygen in human tumors: Correlations between methods of measurement and response to therapy. *Radiat Res* 136:422–434.
- Thomas SR. 1988. The biomedical applications of Fluorine-19 NMR. In: Partain CL, Price RR, Patton JA, Kulkarni MV, James AEJ, editors. *Magnetic resonance imaging*. London: W.B. Saunders Co. p 1536–1552.
- Wouters BG, Brown JM. 1997. Cells at intermediate oxygen levels can be more important than the “hypoxic fraction” in determining tumor response to fractionated radiotherapy. *Radiat Res* 147:514–520.
- Zhao D, Hahn EW, Constantinescu A, Mason RP. 2000. A comparison of oxygen dynamics during respiratory challenge in two Dunning prostate tumor sublines having diverse Tpts: Radiation Research Soc. Meeting. Albuquerque, NM.
- Zhao D, Constantinescu A, Jiang L, Hahn EW, Mason RP. 2001a. Prognostic radiology: Quantitative assessment of tumor oxygen dynamics by MRI. *Am J Clin Oncol* 24:462–466.
- Zhao Z, Constantinescu A, Hahn EW, Mason RP. 2001b. Tumor oxygen dynamics with respect to growth and respiratory challenge: Investigation of the Dunning prostate R3327-HI tumor. *Radiat Res* 156:510–520.
- Zhao D, Constantinescu A, Hahn EW, Mason RP. 2002a. Measurement of tumor oxygen dynamics predicts beneficial adjuvant intervention for radiotherapy in Dunning prostate R3327-HI tumors. *Radiat Res* (in press).
- Zhao D, Constantinescu C, Hahn EW, Mason RP. 2002b. Differential oxygen dynamics in two diverse Dunning prostate R3327 rat tumor sublines (MAT-Lu and HI) with respect to growth and respiratory challenge. *Int J Radiat Oncol Biol Phys* 53:744–756.